Supplementary Information

Magic Number Pt_{13} and Misshapen Pt_{12} Clusters: Which one is the Better Catalyst?

Takane Imaoka[1], Hirokazu Kitazawa[1], Wang-Jae Chun[2], Saori Omura[1], Ken Albrecht[1], Kimihisa Yamamoto[1]*

[1]Chemical Resources Laboratory, Tokyo Institute of Technology, Yokohama 225-8503, Japan. [2]Graduate School of Arts and Sciences, International Christian University, Mitaka, Tokyo 181-8585, Japan.

*e-mail: yamamoto@res.titech.ac.jp

XAFS analysis. XAFS spectra were analyzed by using REX2000, an EXAFS analysis program package (Rigaku Co., Japan).[1] EXAFS oscillations were extracted using spline smoothing with a Cook-Sayers criterion.[2] The oscillation was normalized using an edge height with its energy dependence expressed using a Victoreen equation. The origin for the photoelectron kinetic energy was set at the inflection point of the absorption edge. To estimate coordination numbers and bond distance the EXAFS data were curve fitted in a *k* space with the following equation:

$$k^3\chi(k) = \sum_i \frac{k_i^2 N_i F_i(k) exp^{(-2\sigma_i^2 k_i^2)} \sin\left[2k_i r_i + \phi_i(k)\right]}{r_i^2}$$

where N_i, r_i and σ_i are coordination number, interatomic distance, and Debye-Waller factor for the *i*-th shell, respectively. They were optimized during the curve-fitting procedure. $F_i(k)$ and $\phi_i(k)$ are amplitude and phase-shift functions, respectively. The

theoretical amplitude and phase shift functions for Pt-Pt, Pt-C, Pt-N were calculated by FEFF 8.4 code.[3] The E_0 was optimized for each shell using following equation.

$$k = \sqrt{k'^2 - \frac{2m}{\hbar^2}\Delta E_0}$$

The number of independent parameters allowed for the curve fitting process given by the following equation.[4]

$$M = \frac{2\Delta k \Delta r}{\pi} + 2$$

The degree of the curve fitting was evaluated by the R_f factor defined as follows.

$$R_f = \sqrt{\frac{k^n \chi_{obs}(k) - k^n \chi_{cal}(k)}{k^n \chi_{obs}(k)}}$$

The XANES region of the Pt L_3 and L_2 absorption edges were used to determine the fractional d-electron occupancy of the Pt atoms in the samples by white line analysis. Mansour et al. have reported that comparison of the white line intensities of a sample with those of a reference metal foil provides a measure of the fractional d-electron vacancy, f_d, of the absorber atoms in the sample.[5]

f_d is given by following equation

$$f_d = (\Delta A_3 + 1.11\Delta A_2)/(A_{3,r} + 1.11A_{2,r})$$

where $A_{3,r}$ and $A_{2,r}$ represent the area under the white line at the L_3 and L_2 edge of the reference foil spectrum, respectively. $\Delta A_{3,r}$ and $\Delta A_{2,r}$ represent the difference of the area under the white line at the L_3 and L_2 edge of the samples.

The total number of unoccupied d-states per Pt atom in the samples was also estimated by following equation,

$$\left(h_{\mathrm{J}}\right)_{\mathrm{t,s}} = (1.0 + \mathrm{f_d})\left(h_{\mathrm{J}}\right)_{\mathrm{t,r}}$$

where $(h_J)_{t,s}$ and $(h_J)_{t,r}$ represent the total value of the sample and the reference, respectively. The $(h_J)_{t,r}$ for Pt foil was fixed to 0.3.[6] The equation indicates that a large $(h_J)_{t,s}$ value means a smaller d-electron density and an increased d band vacancy as compared to those for Pt foil (bulk).

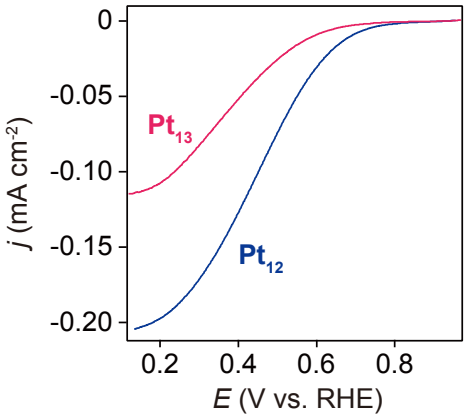

Figure S1. Rotating disk Voltammograms of the Pt_{12} (25.7 ng) and Pt_{13} (27.9 ng) modified electrodes in oxygen-saturating electrolyte (aqueous solution of 0.1 mol L^{-1} $HClO_4$) at the rotating rate of 300 rpm. In order to determine the mass-activity, these voltammograms were measured with least amounts of the platinum catalysts at much below the O_2-diffusion limit.

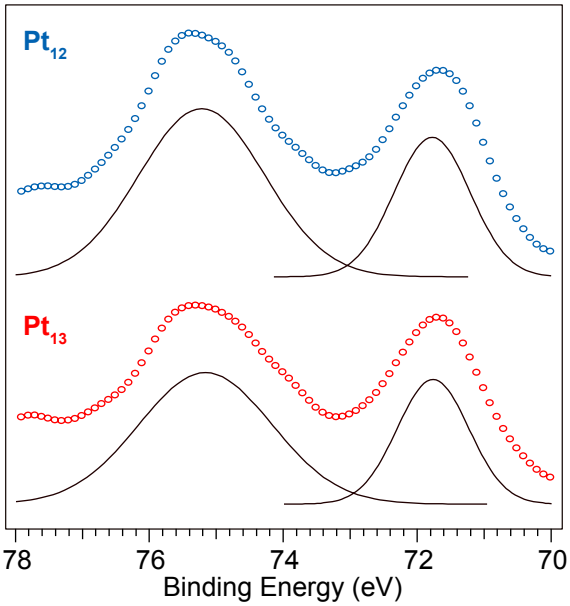

Figure S2. X-ray photoelectron spectra of Pt_{12} and Pt_{13}. The binding energies of the $Pt4f_{7/2}$ peaks for Pt_{12} and Pt_{13} were both 71.8 eV, obtained by the deconvolution (lines) of the experimental data (circle).

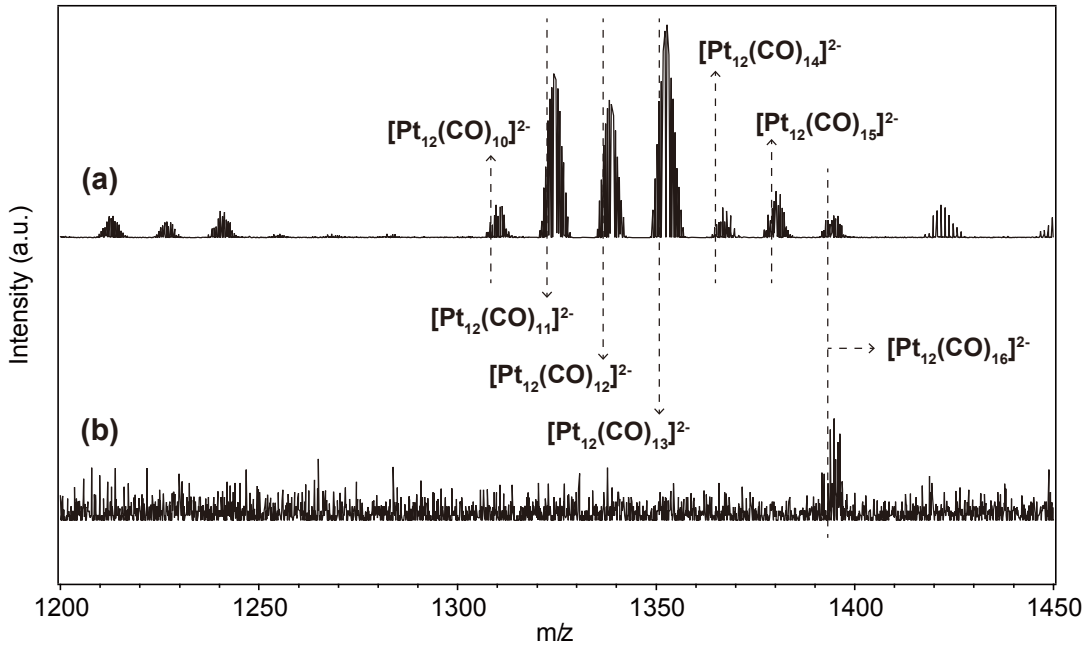

Figure S3. Negative-mode ESI-TOF-MS spectra of the Pt_{12}.carbonyl clusters synthesized with TPM-DPA. Each spectrum was measured with different cone voltages, (a) 75 V, (b) 50V.

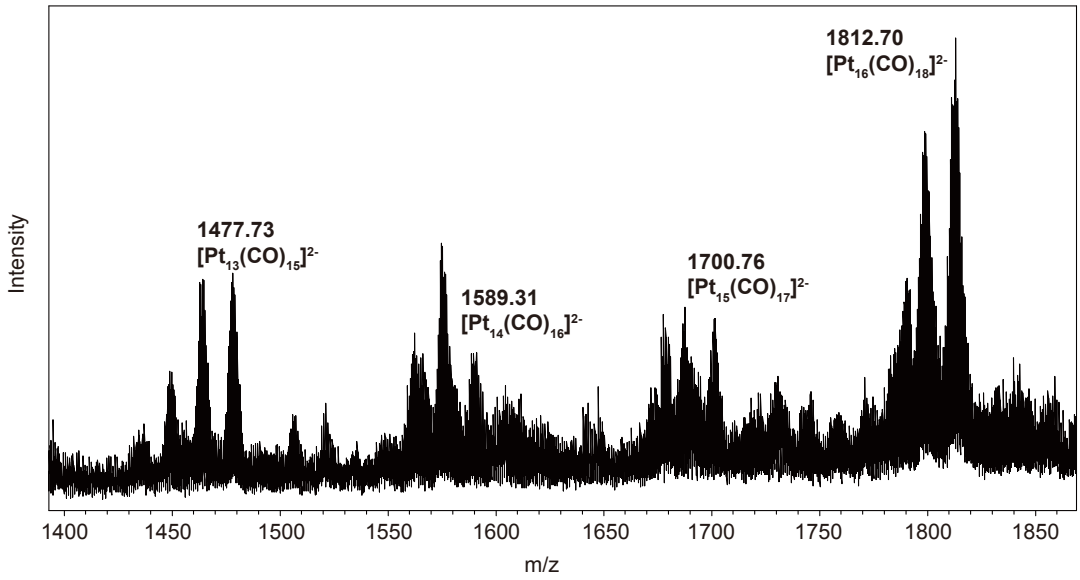

Figure S4. A negative-mode ESI-TOF-MS spectrum of the platinum clusters synthesized with PyTPM-DPA. The platinum chloride was overloaded.

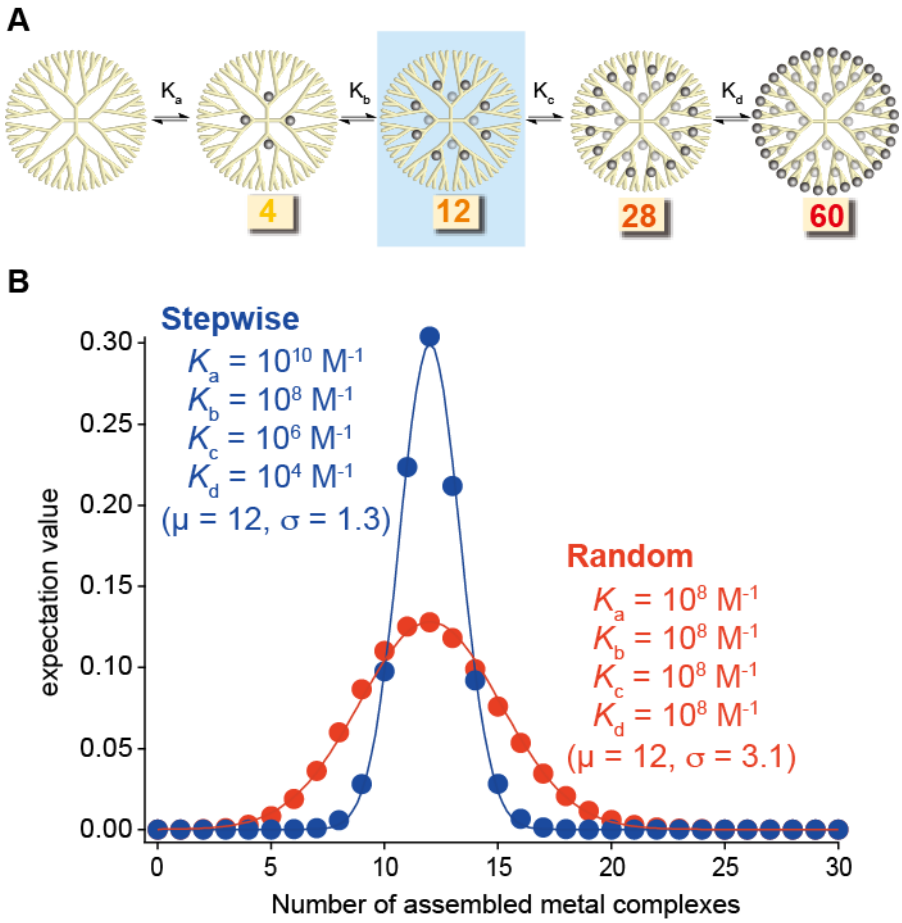

Figure S5. (A) Schematic representation of the stepwise complexation, (B) Calculated distributions in the number of the assembled metal ($PtCl_4$) in a dendrimer template assuming that a 12 equimolar amount of the metal was added. If the association constants were identical for every coordination site in the dendrimer, the profile becomes a Gaussian-type normal distribution with a relatively large standard deviation ($\sigma = 3.1$). In contrast, if a stepwise complexation was assumed (2-orders of magnitude difference between each neighboring layer) as the previous result,[7] the standard deviation became much smaller ($\sigma = 1.3$). The average number (μ) was 12 in both cases.

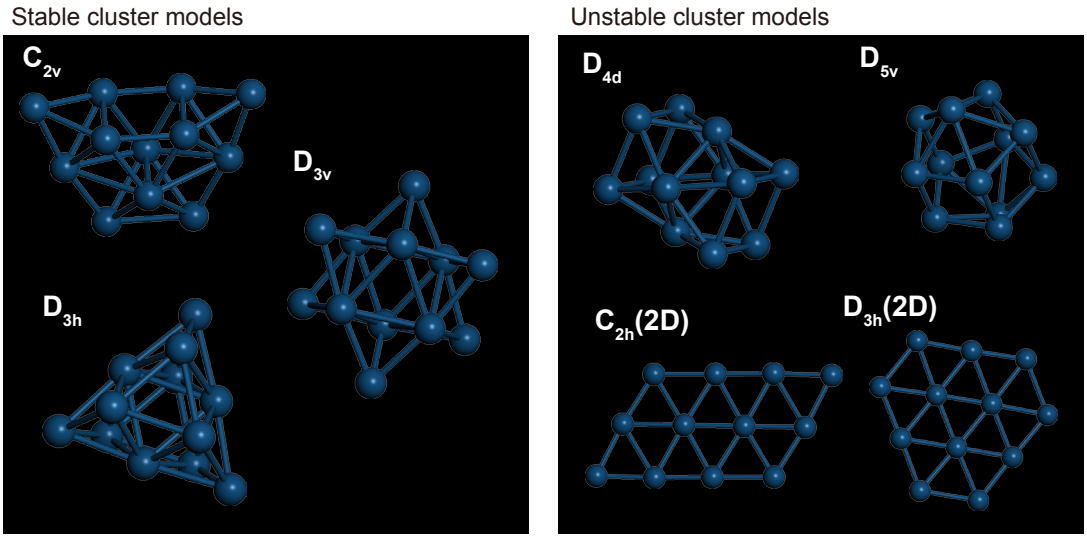

Figure S6. The expected cluster models of Pt_{12} optimized by DFT calculations. These clusters were categorized as stable ($\Delta\Delta G$ from the most stable cluster is less than 10 kcal mol^{-1}) and unstable ($\Delta\Delta G$ = 10 ~ 40 kcal mol^{-1}).

Table S1. Fractional d-electron (f_d) vacancy and the total number of unoccupied d-states per Pt atoms calculated from the XANES data shown in Figure 5.

Sample	f_d	(h_J)t,s
Pt foil	0.00	0.30
Pt_{12}	0.29	0.39
Pt_{13}	0.36	0.41

Table S2. Curve fitting results of the EXAFS with an additional Pt-C or Pt-N shell.

sample	bond	N	r / Å	ΔE_0 / eV	$\Delta\sigma^2$ / 10^{-3} Å^2	R_f / %
Pt foil*	Pt-Pt	12	2.77	*n/a*	*n/a*	*n/a*
Pt_{12}	Pt-Pt	5.2 ± 1.3	2.74 ± 0.02	7.0 ± 3.9	8.8 ± 0.2	0.2
	Pt-C	2.3 ± 0.9	2.46 ± 0.02	-14.3 ± 5.1	1.5 ± 2.7	
Pt_{13}	Pt-Pt	6.5 ± 1.4	2.75 ± 0.01	11.4 ± 2.8	9.2 ± 0.1	0.1
	Pt-C	3.3 ± 1.1	2.43 ± 0.02	-20.8 ± 5.1	4.2 ± 1.2	
Pt_{12}	Pt-Pt	4.7 ± 1.2	2.74 ± 0.01	7.3 ± 3.6	8.3 ± 0.2	0.2
	Pt-N	2.3 ± 0.8	2.44 ± 0.02	-10.9 ± 5.1	2.1 ± 1.6	
Pt_{13}	Pt-Pt	6.1 ± 1.3	2.75 ± 0.01	11.4 ± 2.8	9.0 ± 0.1	0.1
	Pt-N	3.1 ± 1.0	2.42 ± 0.02	-15.5 ± 4.7	4.8 ± 1.0	

*Crystallographic data

** Fourier filtering region is limited where Δr = 1.75 ~ 3.04 Å for Pt_{12}, Δr = 1.65 ~ 3.04 Å for Pt_{13}.

Table S3. Calculated stabilities and oxygen binding energies to the surfaces of the possible clusters shown in Figure S6.

model	N(Pt-Pt)	$\Delta\Delta G^0$ (kcal mol^{-1})[a]	ΔE (eV)[b]
C_{2v}	30	0	0.386, 0.276, -0.812, 0.162, 0.285, 0.266
D_{3v}	30	-6.83	-1.333, -0.022, 3.707
D_{3h}	33	-4.10	0.722, 0.930, -1.248
D_{4d}	28	+4.96	0.535, -0.285
D_{5v}	28	+32.9	-0.305
C_{2h}(2D)	23	+40.4	0.084, 0.524, 0.142, 0.665, 0.354, 0.351
D_{3h}(2D)	24	+42.1	0.069, 0.243, 0.454, 0.133

[a]Relative stabilities of the clusters for the C_{2v} cluster calculated by DFT. [b]Oxygen binding energies to each of the nonequivalent 3-fold hollow sites.

References

1. Taguchi, T.; Ozawa, T.; Yashiro, H. *Phys. Scripta* **2005**, *T115*, 205-206.

2. Cook, J. W.; Sayers, D. E. *J. Appl. Phys.* **1981**, *52*, 5024-5031.

3. Ankudinov, A. L.; Ravel, B.; Rehr, J. J.; Conradson, S. D. *Phys. Rev. B* **1998**, *58*, 7565.

4. Stern; E. A. *Phys. Rev. B* **1993**, *48*, 9825–9827.

5. Mansour, A. N.; Cook, J. W.; Sayers, D. E. *J. Phys. Chem.* **1984**, *88*, 2330-2334.

6. Brown, M.; Peierls, R. E.; Stern, D. E. *Phys. Rev. B* **1977**, *15*, 738-744.

7. Yamamoto, K.; Imaoka, T. *Bull. Chem. Soc. Jpn.* **2006**, *79*, 511-526.